

# UCLA

## UCLA Previously Published Works

### Title

Complete topology inversion can be part of normal membrane protein biogenesis

### Permalink

<https://escholarship.org/uc/item/7g0661hz>

### Journal

Protein Science, 26(4)

### ISSN

0961-8368

### Authors

Woodall, Nicholas B  
Hadley, Sarah  
Yin, Ying  
[et al.](#)

### Publication Date

2017-04-01

### DOI

10.1002/pro.3131

Peer reviewed

# Complete topology inversion can be part of normal membrane protein biogenesis

Nicholas B. Woodall, Sarah Hadley, Ying Yin, and James U. Bowie\*

Department of Chemistry and Biochemistry, UCLA-DOE Institute, Molecular Biology Institute, University of California, Los Angeles, California

Received 17 January 2017; Accepted 2 February 2017

DOI: 10.1002/pro.3131

Published online 7 February 2017 proteinscience.org

**Abstract:** The topology of helical membrane proteins is generally defined during insertion of the transmembrane helices, yet it is now clear that it is possible for topology to change under unusual circumstances. It remains unclear, however, if topology reorientation is part of normal biogenesis. For dual topology dimer proteins such as the multidrug transporter EmrE, there may be evolutionary pressure to allow topology flipping so that the populations of both orientations can be equalized. We previously demonstrated that when EmrE is forced to insert in a distorted topology, topology flipping of the first transmembrane helix can occur during translation. Here, we show that topological malleability also extends to the C-terminal helix and that even complete topology inversion of the entire EmrE protein can occur after the full protein is translated and inserted. Thus, topology rearrangements are possible during normal biogenesis. Wholesale topology flipping is remarkable given the physical constraints of the membrane and expands the range of possible membrane protein folding pathways, both productive and detrimental.

**Keywords:** membrane topology; topology flipping; membrane protein folding; topology inversion; topology change; transmembrane helix

## Summary

Once transmembrane segments are inserted in a particular topology, the bilayer would appear to present a severe challenge for subsequent topology changes. Nevertheless, topology changes have been documented when the protein or membrane is distorted. Here, we find that full topological inversion of a membrane protein consisting of four transmembrane helices can occur under normal physiological conditions.

The lipid bilayer presents an apolar barrier to the transport of polar molecules. Even the simple process of lipid flip-flop, moving the lipid headgroup from one bilayer leaflet to another, is associated

with a high energetic barrier. For example, the half-life for flip-flop of phosphatidylcholine lipids can range from hours to days.<sup>1</sup> Thus, models of membrane protein biogenesis generally assume that transmembrane helix topology is fixed upon initial insertion by the translocon, largely defined by the positive inside rule.<sup>2,3</sup> Nevertheless, it is now clear that topology changes are possible.

To our knowledge the first evidence for post-insertion topology changes came from the Skach group, who employed an *in vitro* transcription/translation system to study the topology of aquaporin-1 during biogenesis.<sup>4</sup> When aquaporin-1 was expressed in truncated forms as a proxy for early insertion intermediates, the protein was found inserted in a non-native topology that would need to be subsequently resolved upon insertion of the full protein. In these experiments, however, it remains unclear whether the incorrect topology of these truncated forms reflect true kinetic intermediates along

Additional Supporting Information may be found in the online version of this article.

\*Correspondence to: James U. Bowie, Boyer Hall, University of California, Los Angeles, 611 Charles E Young Dr. E, Los Angeles, CA 90095-1570. E-mail: bowie@mbi.ucla.edu

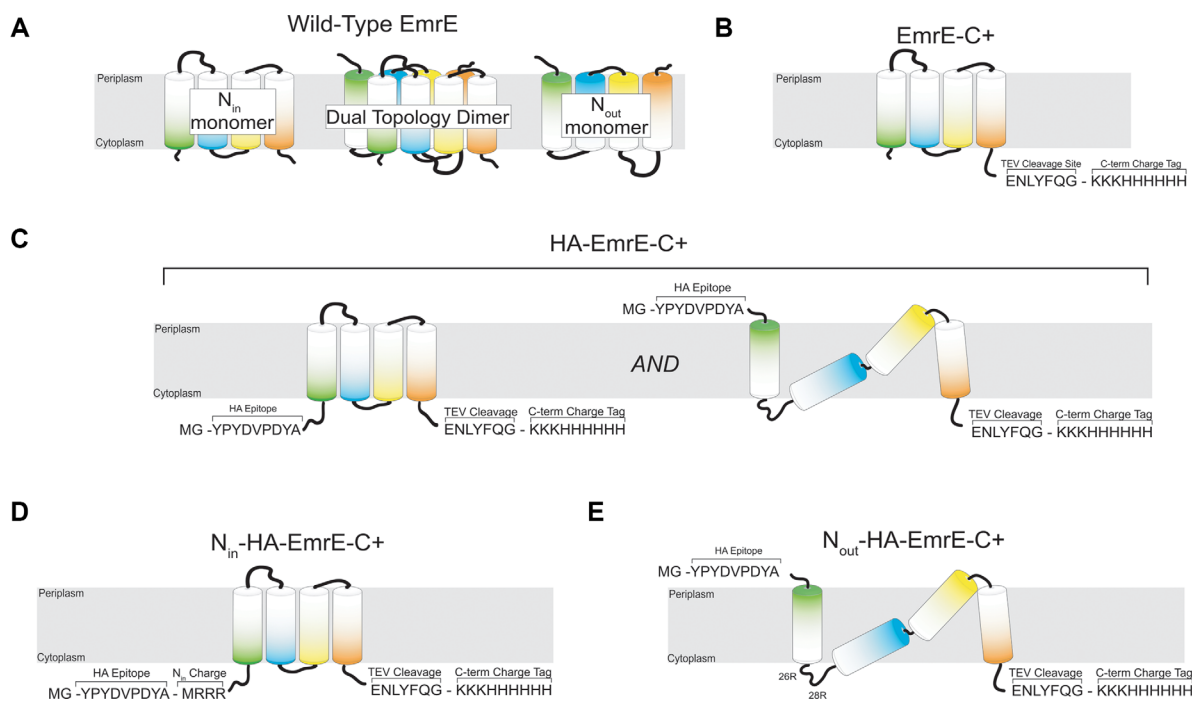


**Figure 1.** EmrE Constructs and Topology Models. **(A)** Wild-Type EmrE is composed of opposite topology monomers with four transmembrane helices that form a dual-topology dimer. **(B)** The construct EmrE-C+ consists of a wild-type N-terminus and a C-terminal positive-charge tag behind a TEV protease cleavage site. The topology of this construct has been previously shown to be  $N_{in}/C_{in}$ .<sup>10</sup> **(C)** HA-EmrE-C+ adds an HA-epitope tag to the N-terminus of EmrE-C+. The addition of the N-terminal HA epitope traps the N-terminus of EmrE in its initially inserted topology.<sup>10</sup> The C-terminal positive charges enforce a cytoplasmic C-terminus. The distorted  $N_{out}/C_{in}$  topology model shown is one of many possible ways to generate an  $N_{out}/C_{in}$  topology. **(D)**  $N_{in}$ -HA-EmrE-C+ adds three arginine residues to the N-terminus of HA-EmrE-C+ driving the formation of a homogenous  $N_{in}/C_{in}$  topology.<sup>10</sup> **(E)**  $N_{out}$ -HA-EmrE-C+ adds two arginine mutations in the first loop of HA-EmrE-C+ driving the formation of a homogenous distorted  $N_{out}/C_{in}$  topology of  $N_{out}$ -HA-EmrE-C+.<sup>10</sup>

the natural folding pathway or the accumulation of an off-pathway form when translation is halted prematurely.

The Dowhan group has shown that the topology of lactose permease undergoes truly remarkable changes upon variation of phosphatidylethanolamine in the membrane, involving complete topology changes of six transmembrane helices in the N-terminal domain.<sup>5–9</sup> Moreover, these dramatic topology changes are reversible, depending on the lipid composition.

EmrE is a multi-drug resistance transporter that also exhibits topological malleability. EmrE consists of four transmembrane helices, and the active form of EmrE is a dual topology dimer in which the subunits have opposite topologies [Fig. 1(A)], with one subunit in an N-terminal inside/C-terminal inside ( $N_{in}/C_{in}$ ) orientation and the other in an  $N_{out}/C_{out}$  orientation.<sup>11,12</sup> A parallel dimer can also form, however.<sup>13–19</sup>

The wild-type sequence of EmrE exhibits a weak positive-charge bias across its transmembrane helices that allows biogenesis in both topologies in accordance with the positive-inside rule that positive-charges are preferred in the cytoplasm.<sup>20</sup> The von Heijne group showed that when positively-charged residues were placed at the C-terminus of

EmrE, only an  $N_{in}/C_{in}$  topology remained active, suggesting that distant topology signals at the C-terminus could influence the topology of the N-terminal helices after co-translational insertion.<sup>21</sup> Following on this work, we showed that the first transmembrane helix of EmrE normally inserts in both  $N_{in}$  and  $N_{out}$  orientations,<sup>10</sup> so that C-terminal positive charges direct both an  $N_{in}/C_{in}$  orientation and a distorted  $N_{out}/C_{in}$  orientation. The distorted  $N_{out}/C_{in}$  orientation subsequently flips the N-terminus to a normal  $N_{in}/C_{in}$  topology.<sup>10</sup> Thus, there is some topological malleability.

While amazing topology changes are clearly possible, it remains unclear whether they could be part of a normal membrane protein biogenesis process or if topology rearrangements only happen when membrane proteins are forced into unusual membrane environments or distorted topologies. To test whether topology flipping can occur after EmrE synthesis in a natural membrane environment, we added a set of positive charges at the C-terminus of EmrE that could be subsequently removed by TEV protease. The C-terminal charges provide a strong topological signal that directs the C-terminus into the cytoplasm ( $N_{in}/C_{in}$  or  $N_{out}/C_{in}$  topology).<sup>10</sup> The ability to remove the positive charges after the protein is

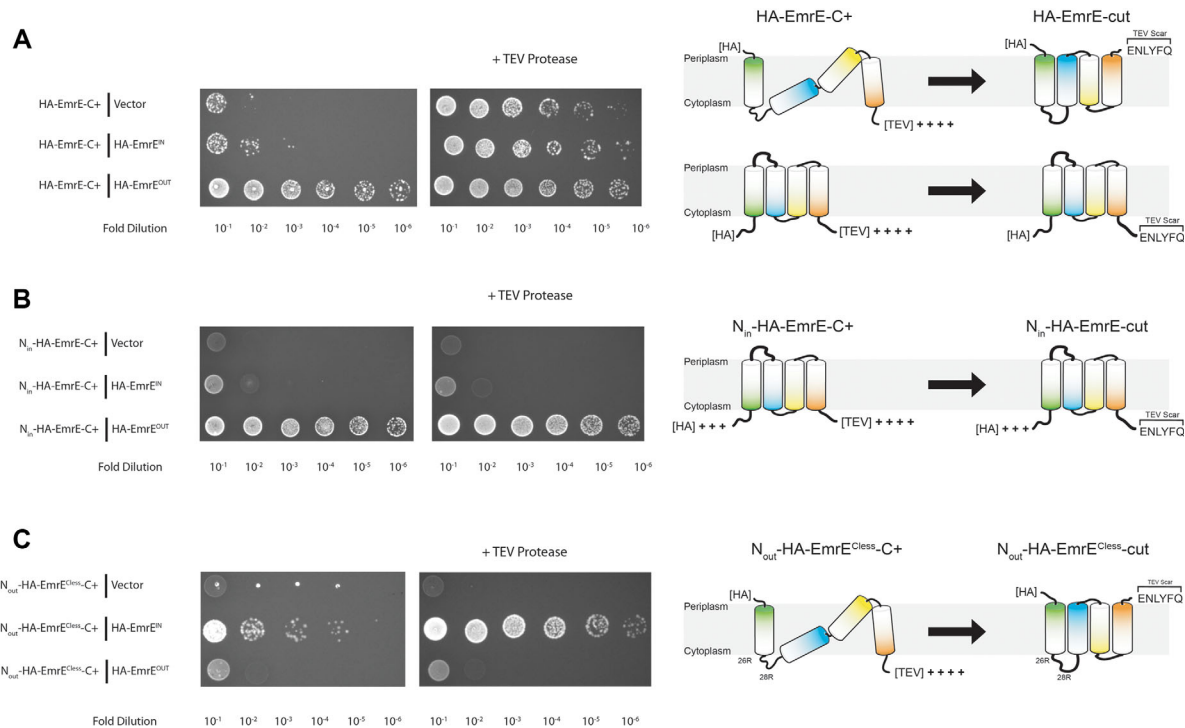


**Figure 2.** Topology Changes Assessed by Ethidium Bromide Resistance. The ability of various combinations of EmrE constructs to grow on plates containing ethidium bromide, in the presence or absence of TEV protease co-expression. Resistance to ethidium bromide is assessed by growth of the indicated dilution of a stationary phase culture. Cartoons at the right present topological models consistent with the results. **(A)** Analysis of HA-EmrE-C+ **(B)** Analysis of  $N_{in}$ -HA-EmrE-C+ **(C)** Analysis of  $N_{out}$ -HA-EmrE<sup>Cless</sup>-C+.

made allows us to observe whether the initially set topology can change after cleavage. We find that after subsequent cleavage of the C-terminal positive charges, the entire subunit is indeed free to invert in the membrane.

## Results and Discussion

### Protein constructs employed in this work

To probe the topological malleability of EmrE, we employed a set of protein constructs shown in Figure 1. The central experimental construct, EmrE-C+, adds a TEV cleavage site, followed by a C-terminal positive-charge tag, KKKHHHHHH [Fig. 1(B)]. The charges provide a strong topology signal that directs both the N and C-termini into the cytoplasm ( $N_{in}/C_{in}$  topology).<sup>10</sup> The TEV site provides a method to cut the tag off, thereby removing the topology signal and allowing us to test whether topology flipping can occur after charge removal. HA-EmrE-C+ adds an HA epitope tag at the N-terminus [Fig. 1(C)]. As shown previously, this construct inserts into the membrane in both a normal  $N_{in}/C_{in}$  topology and a distorted  $N_{out}/C_{in}$  topology, and the HA tag blocks subsequent topology flipping at the N-terminus.<sup>10</sup>  $N_{in}$ -HA-EmrE-C+ adds a few N-terminal positive charges to generate a pure  $N_{in}/C_{in}$  topology [Fig. 1(D)] while  $N_{out}$ -HA-EmrE-C+ adds positive charges

to the first extra-membrane loop to generate a pure  $N_{out}/C_{in}$  distorted topology [Fig. 1(E)].<sup>10</sup>

### Topological malleability at the C-terminus

We had previously shown that an  $N_{out}/C_{in}$  topology can be resolved to an  $N_{in}/C_{in}$  topology indicating that the N-terminal helix of EmrE can flip. To further explore the topological malleability of EmrE, we examined whether the C-terminus can flip from a distorted  $N_{out}/C_{in}$  topology to a regular  $N_{out}/C_{out}$  topology. We employed the HA-EmrE-C+ construct that contains an HA epitope which blocks N-terminal topology rearrangements so that it inserts in two locked topologies:  $N_{in}/C_{in}$  and distorted  $N_{out}/C_{in}$  [Fig. 1(C)].

The presence of functional EmrE can easily be assessed *in vivo* by resistance of *E. coli* cells to ethidium bromide (EtBr), which is pumped out of the cell by an active EmrE. Since EmrE requires both topological forms to be functional, the topology of a particular construct can be assessed by co-expression with variants that are locked in a single topology by the strategic placement of positively charged residues ( $N_{out}/C_{out}$ : HA-EmrE<sup>OUT</sup> and  $N_{in}/C_{in}$ : HA-EmrE<sup>IN</sup>).<sup>10,20</sup> EtBr resistance occurs when both topologies are present, creating an active dimer.

As shown in Figure 2(A), HA-EmrE-C+ by itself shows low EtBr resistance which is not complemented

by the HA-EmrE<sup>IN</sup> construct, but is complemented by the HA-EmrE<sup>OUT</sup> construct, indicating that HA-EmrE-C+ cannot generate a proper N<sub>out</sub>/C<sub>out</sub> topology. When HA-EmrE-C+ is co-expressed with TEV protease, however, EtBr resistance is dramatically enhanced as would be expected if the C-terminus of the N<sub>out</sub>/C<sub>in</sub> topological form flipped to an N<sub>out</sub>/C<sub>out</sub> topology and dimerizes with the N<sub>in</sub>/C<sub>in</sub> topology of HA-EmrE-C+ [Fig. 2(A)].

To assess which topological form of HA-EmrE-C+ was undergoing a topology change, we examined the ability of TEV protease cleavage to activate the topology locked variants N<sub>in</sub>-HA-EmrE-C+ and N<sub>out</sub>-HA-EmrE<sup>Cless</sup>-C+. In N<sub>out</sub>-HA-EmrE<sup>Cless</sup>-C+ we changed the native cysteine residues to alanine because, for unknown reasons, the native cysteine residues were toxic in this construct alone (Supporting Information Fig. S1). As shown in Figure 2, TEV protease co-expression failed to activate these constructs when expressed alone as the mutated positive charges direct each protein to a single topological form.<sup>10</sup> The N<sub>in</sub>/C<sub>in</sub> topology of N<sub>in</sub>-HA-EmrE-C+ only restores EtBr resistance when co-expressed with HA-EmrE<sup>OUT</sup> regardless of TEV protease expression suggesting that the N<sub>in</sub>/C<sub>in</sub> of HA-EmrE-C+ does not change topology [Fig. 2(B)]. However, after TEV protease co-expression and removal of the C-terminal positive charges, the N<sub>out</sub>/C<sub>in</sub> distorted topology of N<sub>out</sub>-HA-EmrE<sup>Cless</sup>-C+ appears to regain a viable N<sub>out</sub>/C<sub>out</sub> topology since it can be complemented with HA-EmrE<sup>IN</sup> [Fig. 2(C)]. These results suggest that the C-terminus can be driven to move from the cytoplasm to the periplasm.

### **Direct observation of topology changes after cleavage**

To validate the indirect topology measurements from the ethidium bromide resistance phenotypic assay, we used the substituted cysteine accessibility method (SCAM) to directly measure topology.<sup>22</sup> SCAM ascertains whether a single introduced cysteine resides in either the cytoplasm or the periplasm by assessing its reaction with a membrane-impermeable reagent, in this case, 4-acetamido-4'-maleimidylstilbene-2,2'-disulfonic acid (AMS). AMS is first incubated with whole cells, allowing it to react with periplasmic cysteine residues. After AMS is washed away, membranes are solubilized in detergent and a biotinylation reagent, 3-(*N*-maleimido-propionyl)-biocytin (MPB) is added to react with any free cysteine residues that have not been blocked by AMS. In this way, cysteine residues in the periplasm will be modified by AMS and cysteine residues in the cytoplasm will be biotinylated with MPB. We can then differentiate the two cases, by observing whether the EmrE construct gel-shifts with the addition of avidin. Since the biotinylation reaction is somewhat variable, we run a biotinylation only

control with every sample to assess the percent change in biotinylation due to the AMS pre-reaction, which we term AMS response (see Methods). Control experiments indicate that a cytoplasmic cysteine can be fully protected from AMS (0% AMS response), fully periplasmic cysteines are highly, but not completely reactive with AMS (~75% response), and mixed topologies generate an intermediate response (Supporting Information Fig. S2).<sup>10</sup>

The HA epitope cannot cross the membrane, trapping the N-terminus of EmrE in these experiments in its initially inserted topology.<sup>10</sup> As such, we can monitor the movement of the C-terminal half of EmrE after TEV protease cleavage. As described previously, we changed all the native cysteine residues in EmrE to alanine (C39A, C41A, C95A) creating EmrE<sup>Cless</sup>, which eliminates background reactions with the maleimide reagents (Supporting Information Fig. S3). The T108C mutation allows us to monitor the movement of the C-terminus of EmrE in the constructs HA-EmrE<sup>Cless</sup>-C+, N<sub>in</sub>-HA-EmrE<sup>Cless</sup>-C+ and N<sub>out</sub>-HA-EmrE<sup>Cless</sup>-C+. In our previous work, we established that when T108C is adjacent to the C-terminal positive charges, it is always cytoplasmic.<sup>10</sup>

When the EmrE constructs are co-expressed with TEV protease, the cleaved form of EmrE is resolved on the gel from the full length form of EmrE allowing both the cut and full length topologies to be assessed at the same time. In line with the previous results T108C is cytoplasmic in the full length constructs as indicated by the low AMS response in the constructs HA-EmrE<sup>Cless</sup>-C+ T108C ( $-3\% \pm 8\%$ ), N<sub>in</sub>-HA-EmrE<sup>Cless</sup>-C+ T108C ( $3\% \pm 2\%$ ) and N<sub>out</sub>-HA-EmrE<sup>Cless</sup>-C+ T108C ( $9 \pm 7\%$ ) (Fig. 3). Once cleaved the distorted topology of N<sub>out</sub>-HA-EmrE<sup>Cless</sup>-C+ T108C re-orientates to move T108C into the periplasm as shown by the increase in the AMS response for N<sub>out</sub>-HA-EmrE<sup>Cless</sup>-C+ T108C after cleavage ( $47\% \pm 17\%$ ) [Fig. 3(A)]. With the N-terminus cytoplasmic in the construct N<sub>in</sub>-HA-EmrE<sup>Cless</sup>-C+ T108C, T108C is already in line with a proper topology for EmrE and we observe no movement across the membrane after cleavage, indicated by an indistinguishable AMS response ( $-1\% \pm 4\%$ ) compared to the full length protein ( $3\% \pm 2\%$ ) [Fig. 3(B)]. HA-EmrE<sup>Cless</sup>-C+ T108C which is composed of equal portions N<sub>in</sub> and N<sub>out</sub> shows movement into periplasm as well with an increased AMS response upon cleavage (increase from  $-3\% \pm 8\%$  to  $38\% \pm 12\%$ ), most likely originating from the N<sub>out</sub>/C<sub>in</sub> topology monomers [Fig. 3(C)].

### **Full topology inversion**

The results so far and our prior work<sup>10</sup> indicate that the N- and C-terminal ends of EmrE can change topologies in response to a distorted topology at the other end of the protein. But if the protein is

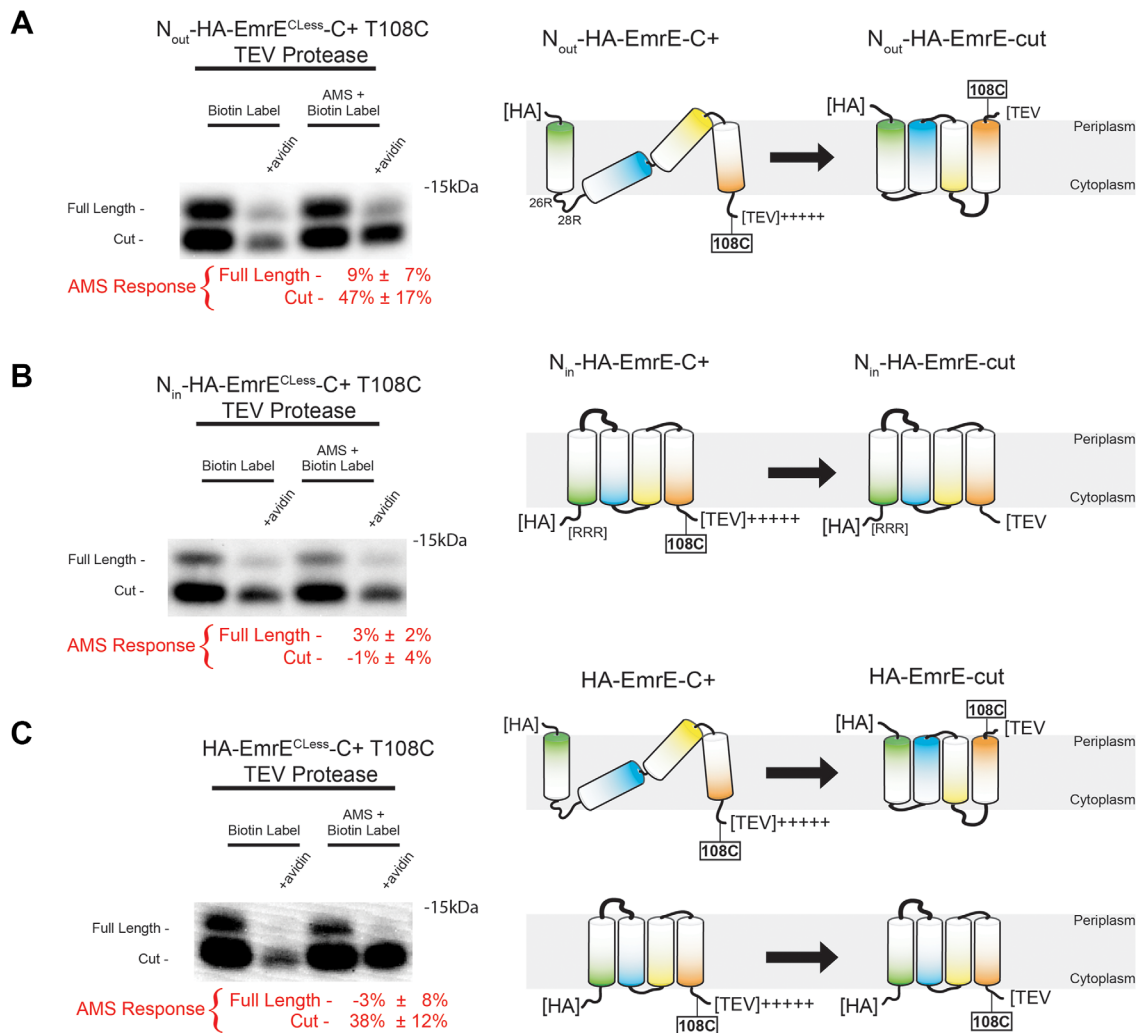


**Figure 3.** Analysis of C-terminal Topology Changes. SCAM analysis of the C-terminal topology of EmrE constructs before and after cleavage by TEV protease. The representative western blots show the ability of avidin to gel-shift biotinylated EmrE with or without prior reaction with AMS as indicated. Only the non-avidin shifted bands are shown. Protection from biotinylation is quantified as the AMS response (see Methods). The mean AMS response and standard deviation of three separate experiments are shown below each representative blot. Proposed topology models consistent with the cysteine SCAM data are shown on the right. **(A)** Analysis of the  $N_{out}$ -HA-EmrE<sup>C<sup>Less</sup>-C+</sup> construct. In the full length distorted topology construct  $N_{out}$ -HA-EmrE<sup>C<sup>Less</sup>-C+</sup>, T108C is completely cytoplasmic as indicated by the negligible AMS response. After TEV protease cleavage,  $N_{out}$ -HA-EmrE<sup>C<sup>Less</sup></sup> undergoes a topology change with some of the T108C residues moving into periplasm as indicated by the increased AMS response of the cut form. **(B)** Analysis of the  $N_{in}$ -HA-EmrE<sup>C<sup>Less</sup>-C+</sup> construct. In the full length and cut versions of  $N_{in}$ -HA-EmrE<sup>C<sup>Less</sup>-C+</sup>, T108C is completely cytoplasmic as indicated by the negligible AMS response. Topology changes upon cleavage are not observed. **(C)** Analysis of the HA-EmrE<sup>C<sup>Less</sup>-C+</sup> T108C construct. HA-EmrE<sup>C<sup>Less</sup>-C+</sup> adopts a mixed topology, composed equally of  $N_{in}$  and  $N_{out}$  forms.<sup>10</sup> In the full length construct, T108C is cytoplasmic as measured by the low AMS response for both topological forms. After TEV protease cleavage, however, a fraction of the T108C moves into the periplasm as indicated by the increase in AMS response.

inserted in a normal topology with no topology distortions to drive changes, would it still flip? To test this possibility we removed the HA epitope which blocks topology flipping at the N-terminus,<sup>10</sup> creating the construct EmrE-C+ (Fig. 1). EmrE-C+ adopts a uniform  $N_{in}/C_{in}$  topology.<sup>10</sup> Removing the C-terminal positive charges by TEV protease cleavage would thereby eliminate any topological determinants and free the protein to flip in the membrane, if possible.

As seen in Figure 4(A), cells expressing EmrE-C+ grow poorly on EtBr, consistent with insertion in a single  $N_{in}/C_{in}$  topology without an  $N_{out}/C_{out}$  partner to form an active dimer.<sup>10</sup> Co-expressing EmrE-C+ with an  $N_{in}/C_{in}$  single topology EmrE mutant, HA-EmrE<sup>IN</sup>, does not restore growth on EtBr, further indicating that EmrE-C+ and HA-EmrE<sup>IN</sup> are in the same topology [Fig. 4(A)]. However, when EmrE-C+ was co-expressed with the single topology HA-EmrE<sup>OUT</sup> variant, EtBr resistance is

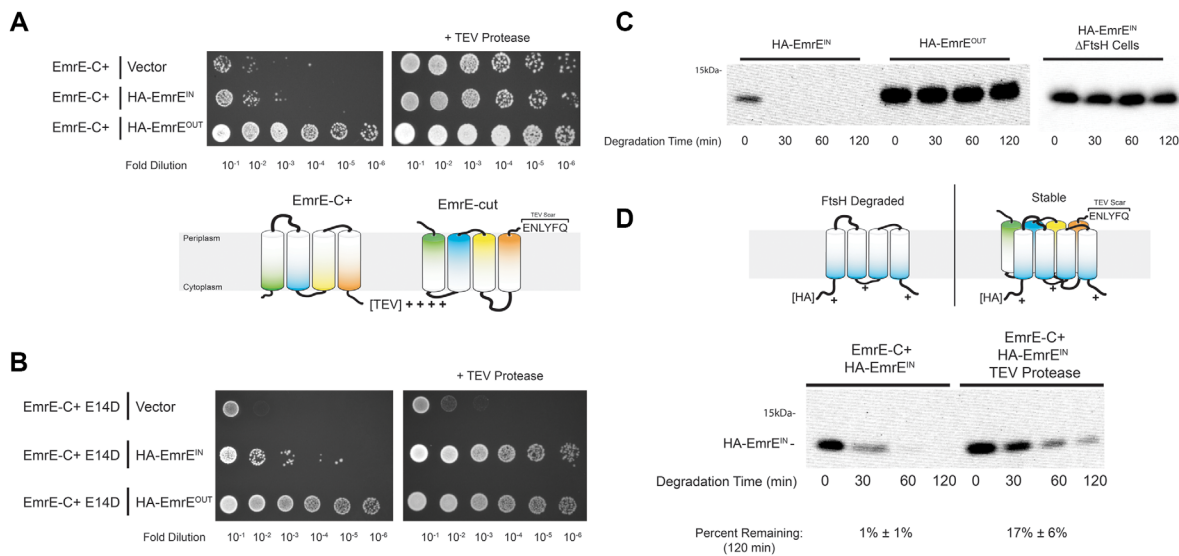


**Figure 4.** Full Topology Inversion of EmrE-C+. **(A)** EmrE-C+ topology before and after cleavage by TEV protease assessed by ethidium bromide resistance, as described in Figure 2. A topological interpretation of the results is shown below the growth results. **(B)** EmrE-C+ E14D topology before and after cleavage by TEV protease assessed by ethidium bromide resistance, as described in Figure 2. **(C)** Degradation of EmrE constructs by FtsH protease. Western blots show EmrE levels after protein synthesis is halted by the addition of erythromycin (degradation time zero). HA-EmrE<sup>IN</sup> and HA-EmrE<sup>OUT</sup> were expressed in FtsH+ cells for the left two panels. The third panel shows that HA-EmrE<sup>IN</sup> degradation is largely eliminated in  $\Delta$ FtsH cells. **(D)** Degradation of HA-EmrE<sup>IN</sup> in the presence of uncut EmrE-C+ or cut EmrE-C+. HA-EmrE<sup>IN</sup> is stabilized when EmrE-C+ is expressed with TEV protease, consistent with its ability to change topology after cleavage and bind to HA-EmrE<sup>IN</sup>. The blot shown is representative. The percent of HA-EmrE<sup>IN</sup> remaining after 120 minutes is indicated at the bottom (mean and standard deviation of triplicates).

restored as observed previously.<sup>10,20</sup> Taken together, these results indicate that without removal of the C-terminal positive charges, EmrE-C+ adopts an  $N_{in}/C_{in}$  topology only.

As shown in Figure 4(A), when the TEV protease is co-expressed with EmrE-C+ alone, the EtBr resistance increases dramatically, suggesting that both topologies are present. If so, it would require that cut EmrE-C+ can flip in the membrane after the protein is made in the  $N_{in}/C_{in}$  topology. Co-expression with HA-EmrE<sup>IN</sup> or HA-EmrE<sup>OUT</sup>, does not change the EtBr resistance as EmrE-cut is active alone [Fig. 4(A)].

To further evaluate whether the gain of function occurs simply by removal of the C-terminal positive charges, we employed the active site mutation E14D. The E14D mutation is inactive by itself, but can form an active dimer when paired with a wild-type subunit.<sup>20,23</sup> Thus, we reasoned that if activation occurs upon TEV protease cleavage of a subunit containing an E14D mutation, it must be due to proper pairing with another subunit and not activation of the cleaved subunit itself. As shown in Figure 4(B), both EmrE-C+ E14D and EmrE-cut E14D are inactive since only E14D monomers are present. When EmrE-C+ E14D is co-expressed with HA-EmrE<sup>OUT</sup>, however, a functional dimer of  $N_{in}/C_{in}$  EmrE-C+ E14D and HA-EmrE<sup>OUT</sup> is formed [Fig. 4(B)]. The combination of EmrE-C+ E14D and HA-

EmrE<sup>IN</sup>, fails to yield a productive interaction, as expected, since both subunits are in an  $N_{in}/C_{in}$  orientation. When EmrE-C+ E14D is cleaved by the TEV protease to EmrE-cut E14D, however, activity is restored in the presence of HA-EmrE<sup>IN</sup>, consistent with the ability of EmrE-cut E14D to flip topologies and form an active dimer with HA-EmrE<sup>IN</sup> [Fig. 4(B)].

While the biological phenotypes strongly suggest the EmrE possesses the ability to completely flip topology, we wanted to test the ability at the protein level. The absence of an antibody tag in the EmrE-C+ construct after TEV cleavage, however, precluded the SCAM analysis employed above. We therefore employed an indirect assay that detects anti-parallel dimer formation by protection from intracellular proteolysis. As shown in Figure 4(C), HA-EmrE<sup>IN</sup> construct is degraded at a much higher rate than our HA-EmrE<sup>OUT</sup> mutant despite a difference of only a few topology defining mutations, because the cytoplasmically located FtsH protease can grasp the termini of HA-EmrE<sup>IN</sup>, but not HA-EmrE<sup>OUT</sup>. The half-life of the HA-EmrE<sup>IN</sup> construct is less than 30 min while the EmrE<sup>OUT</sup> construct shows no obvious degradation after 120 min. When HA-EmrE<sup>IN</sup> is expressed in FtsH null cells, its degradation is essentially eliminated, indicating that FtsH is the primary protease responsible for degrading HA-EmrE<sup>IN</sup> [Fig. 4(C)].

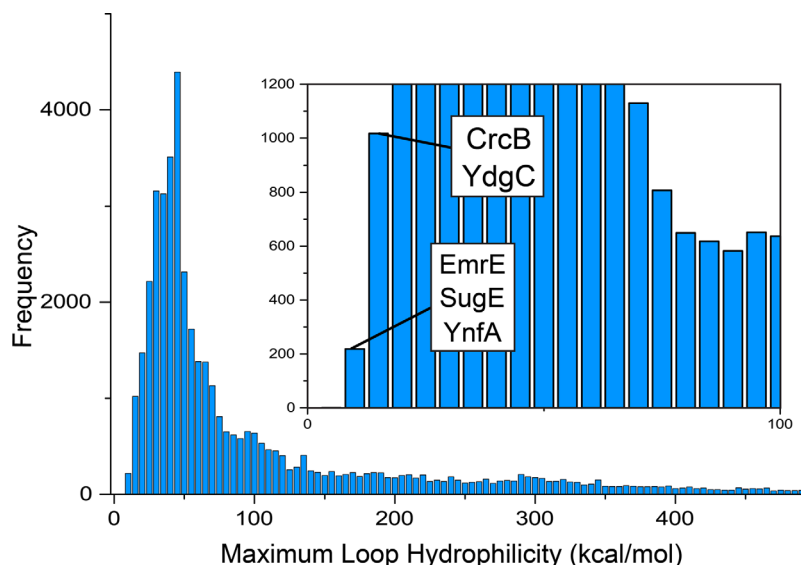


**Figure 5.** Maximum Loop Hydrophilicity Histogram of Membrane Proteins. Each membrane protein with at least three trans-membrane helices in the UniprotKB/Swiss Protein database was analyzed for the maximum hydrophilicity of their extra-membrane segments. The positions of EmrE and other known dual topology proteins identified previously<sup>27</sup> are marked on the inset. The histogram was truncated at 500 kcal/mol.

We previously showed that HA-EmrE-C+ was protected from FtsH proteolysis if it could form an active anti-parallel dimer, presumably because the  $N_{in}/C_{in}$  topological form is stabilized in the dimer, making it immune to FtsH proteolysis.<sup>24</sup> Thus, if EmrE-C+ can change topologies to an  $N_{out}/C_{out}$  state after TEV cleavage, then it should stabilize the  $N_{in}/C_{in}$  construct, HA-EmrE<sup>IN</sup>, which we can monitor using the HA epitope. Indeed, as seen in Figure 4(D), HA-EmrE<sup>IN</sup> has increased stability when co-expressed with EmrE-C+ and the TEV protease (17%  $\pm$  6% remaining after 2 hours of degradation compared to 1%  $\pm$  1% without the TEV protease).

## Conclusion

Our results indicate that EmrE exhibits a high degree of topological malleability. Both the N- and C-termini can change topology independently and the entire protein subunit can flip completely in the membrane. While it is possible that the entire protein flips as a monomer or dimer in a concerted manner, we suggest that the flipping is more likely to occur from the relatively unstable monomeric form in a more piecemeal process. In particular, mechanisms that require the passage of only a single hydrophilic loop at a time should be favored. Our results are largely consistent with the kinetic annealing model of Van Lehn et al., in which EmrE can insert initially in a variety of topologies which can be subsequently resolved into either an  $N_{in}/C_{in}$  or  $N_{out}/C_{out}$  topology.<sup>25</sup> What was not anticipated in the model, however, was that the energy barrier for the kinetic annealing process may be low enough for EmrE to continue in reverse. In particular, if the

distorted topologies such as  $N_{out}/C_{in}$  are not too unfavorable energetically, it is possible that they could be explored with reasonable probability even after correct topologies are achieved, ultimately resolving in an inverted orientation.

The largest energetic barrier for topology flipping would likely be the crossing of the most hydrophilic loop or termini in the protein. Thus we might expect that proteins like EmrE that can flip topologies would experience evolutionary pressure to maintain relatively hydrophobic extra-membrane loops. To test whether EmrE's extra-membrane loops are unusually hydrophobic, we examined the hydrophobicity distribution of the extra-membrane segments. We determined the Maximum Extra-Membrane Hydrophilicity for each protein in the UniprotKB/Swiss Prot database, which we define as the least hydrophobic segment of all the extra-membrane segments in each protein using the biological hydrophobicity scale.<sup>26</sup> The distribution is shown in Figure 5. The hydrophobicity of the most hydrophilic loop of EmrE was 9.23 kcal/mol, which is among the 0.4% least hydrophilic proteins in the database. Thus, the extra-membrane segments of EmrE are indeed unusually hydrophobic. We then searched for other dual topology proteins previously discovered by the von Heijne group (SugE, CrcB, YdgC, YnfA) and found that they also contain unusually hydrophobic extra-membrane segments (Fig. 5).<sup>27</sup> Thus, other dual topology proteins may well be capable of topology flipping.

Evolutionary pressure for topological malleability makes sense for dual topology proteins like EmrE that need both topologies in equal amounts. Thus,



EmrE maintains relatively short loops and is relatively hydrophobic overall. Whether such folding flexibility occurs in other proteins as part of the natural folding process is an open question. Nevertheless, our results indicate that topology flipping not only occurs under aberrant conditions, but also as part of a normal biogenesis of EmrE, so it is reasonable to suppose that topological changes are part of the natural folding process of other membrane proteins as well. We would expect that other proteins identified with unusually hydrophobic loops might be a fertile place to look for topological malleability. Finally, we must consider the possibility that disease-causing mutations could act by blocking topological malleability required during the folding process. Topological changes after insertion seem particularly likely to occur in proteins with reentrant loops like CIC channels<sup>28</sup> and Aquaporins<sup>4</sup> as suggested originally by the Skach group.

## Methods

### Strains and plasmids

The primary EmrE variant constructs were prepared and expressed in pBAD/His A plasmids (Invitrogen) using NcoI/XhoI cut sites as described previously.<sup>10</sup> HA-EmrE<sup>IN</sup> and HA-EmrE<sup>OUT</sup> were co-expressed in a separate pBAD based vector that bears chloramphenicol resistance and a ClodF13-derived CDF replicon (pBAD<sub>CDF</sub>) described previously.<sup>10</sup> The pRK603 plasmid containing the TEV protease for *in vivo* expression and cleavage of substrates was a gift from David Waugh (Addgene plasmid # 8831) as well as the BL21Pro cells that constitutively express the Tet repressor to control TEV cleavage.<sup>29</sup> AR3291 (FtsH null) cells were a gift from the Ogura lab.<sup>30</sup>

### Ethidium bromide resistance assay

*E. coli* BL21Pro cells containing the desired EmrE construct (pBad HisA plasmid), the complementing EmrE construct (Empty vector, HA-EmrE<sup>IN</sup>, HA-EmrE<sup>OUT</sup>) in pBad<sub>CDF</sub>, and TEV protease on the pRK603 plasmid were grown to saturation over ~8 hours at 37°C in LB media containing 100 µg-mL<sup>-1</sup> ampicillin, 50 µg-mL<sup>-1</sup> kanamycin, and 34 µg-mL<sup>-1</sup> chloramphenicol. The saturated cultures were diluted as indicated into LB broth and 5 µL of each dilution was spotted onto an LB agar plate containing 0.2% (w/v) arabinose, 100 µg-mL<sup>-1</sup> ampicillin, 50 µg-mL<sup>-1</sup> kanamycin, 34 µg-mL<sup>-1</sup> chloramphenicol, 100 ng-mL<sup>-1</sup> anhydrotetracycline (if the TEV protease was induced), and 225 µg-mL<sup>-1</sup> of ethidium bromide. For E14D mutant complementation assays, the ethidium bromide concentration was reduced to 150 µg-mL<sup>-1</sup>. The plates were grown at 37°C for 18 hours before they were imaged on a Gel Doc XR+ (Bio-Rad) using the UV light illumination.

### Cysteine-accessibility topology assay

AR3291 (FtsH null) cells bearing the desired plasmids were grown at 25°C in LB media containing 100 µg-mL<sup>-1</sup> ampicillin, 50 µg-mL<sup>-1</sup> kanamycin, and 34 µg-mL<sup>-1</sup> chloramphenicol to an OD<sub>600</sub> of ~0.8, then induced by the addition of arabinose to 0.2% and incubated at 30°C to express the desired EmrE construct and/or TEV protease. EmrE constructs alone were induced for 2 hours and when both the EmrE construct and the TEV protease were present, induction proceeded for 3 hours. 50 mL of the cell culture was collected by centrifugation and the resuspended in 500 µL of 50 mM phosphate buffer [pH 8.0] with 17 mM NaCl. 200 µL of the resuspension was incubated for 10 minutes with or without 2 mM 4-acetamido-4'-maleimidylstilbene-2,2'-disulfonic acid (AMS) (Thermo Fisher Scientific) with gentle mixing the dark. The cells were pelleted by centrifugation and washed twice with ~1 mL of 50 mM phosphate [pH 7.5]. The final pellet was resuspended in ~475 µL in 50 mM phosphate [pH 7.5]. The cells were then lysed by sonication and then centrifuged at 16,000 g for 10 minutes. Membranes were isolated from the supernatant by centrifugation at 160,000 g in a Beckman Coulter Airfuge for 30 minutes. The membranes were solubilized in 1% SDS, 50 mM phosphate [pH 7.0]. The total protein concentration for each sample was determined by the DC protein assay (Bio-Rad) using bovine serum albumin as a standard. An aliquot of the membranes was biotinylated in 200 µL of 150 µM 3-(N-maleimido-propionyl)-biocytin (MPB) (Thermo Fisher Scientific) in 50 mM phosphate [pH 7.0], 1% SDS and 0.5% dimethyl sulfoxide and a final protein concentration of 0.5 mg-mL<sup>-1</sup>, with gentle mixing for 1 hour at 25°C. The protein was then precipitated with ~1.2 mL of acetone and then centrifuged at 16,000 g to remove unreacted MPB. The pellet was then air-dried and resuspended in 200 µL of 1% SDS in 50 mM phosphate [pH 7.0].

To visualize the AMS and MPB labeling by an avidin gel shift, 30 µL of the labeled sample was mixed with 10 µL of 4X loading dye (250 mM tris [pH 6.75], 40% glycerol, 170 mM β-mercaptoethanol). The sample was then split into two 20 µL aliquots and 2 µL of either 20 mM tris [pH 7.5] or 10 mg/mL avidin (Sigma BioUltra) in 20 mM tris [pH 7.5] was added. 12 µL of each sample was then loaded onto a NuPAGE<sup>TM</sup> 12% Bis-Tris gel (Thermo Fisher Scientific) using Accuruler prestained protein ladder (Lambda Biotech). The gel was resolved for 25 minutes at 40 volts followed by 145 minutes at 100 volts. The gel was then washed twice for 15 minutes in distilled water and then transferred to a PVDF membrane using a Pierce Power Blot Cassette (Thermo Scientific) with Pierce 1-Step Transfer Buffer (Thermo Scientific) for 5 minutes at 1.3 Amps.

The blot was rinsed in water and placed into the iBind (Life Technologies) using the associated iBind Solution Kit (Life Technologies) according to the iBind instructions. A 1 mg·ml<sup>-1</sup> stock of monoclonal HA antibody (Sigma #H3663) and a 1 mg·ml<sup>-1</sup> stock of anti-mouse IgG peroxidase conjugate (Sigma #4416) was diluted 1:1250 in iBind solution. After the iBind step (~2.5 hours), the blot was rinsed with water and was visualized on a FluorChem FC2 (Alpha Innotech) CCD imager using the Amersham ECL Prime detection reagent (GE Healthcare) according to the recommended protocol. The intensity of each band was integrated using ImageJ software with general background subtraction taken from a blank area of the blot. The amount of biotinylation for a given sample was determined from the percent difference in integrated intensity from the lane with avidin compared to the lane without avidin. The percent change in biotinylation of the sample with AMS as compared to the sample without is quantified as AMS Response:

$$\text{AMS Response} = \left( \frac{[\% \text{biotinylated no AMS}] - [\% \text{biotinylated AMS}]}{[\% \text{biotinylated no AMS}]} \right) * 100$$

Each topology assay was run in triplicate and the error quantified as the standard deviation between the three measured AMS responses.

#### **EmrE stability assay**

*E. coli* BL21Pro cells containing HA-EmrE<sup>IN</sup> in the pBAD<sup>CDF</sup> plasmid, EmrE-C+ in the pBAD His A plasmid and the TEV protease on the pRK603 vector were grown in LB media to ~0.6 OD<sup>600</sup> and induced at 30°C for 2 hours. To stop protein synthesis, 350 μg·mL<sup>-1</sup> of erythromycin was then added, denoting time zero in the degradation assay. Aliquots of each culture were taken at the respective time points. The cells were then lysed by sonication in 50 mM phosphate buffer [pH 7.5] and then centrifuged at 16,000 *g* for 10 minutes. Membranes were isolated by the centrifuging the supernatant at 160,000 *g* in the Beckman Coulter Airfuge for 30 minutes. The membranes were solubilized in 1% SDS, 50 mM phosphate [pH 7.0]. The total protein concentration for each sample was determined by the DC protein assay (Bio-Rad) using bovine serum albumin as the standard. The total protein concentration was adjusted to 1 mg·mL<sup>-1</sup> and a 15 μL aliquot was mixed with 5 μL 4X SDS loading dye (250 mM tris [pH 6.75], 40% glycerol, 170 mM β-mercaptoethanol) and then 15 μL of the mixture was loaded into each well. The gel separation and western blot were performed as described above. The HA-EmrE<sup>IN</sup>/EmrE-C+ combinations with or without the TEV protease were performed in triplicate. The error for the

percent of HA-EmrE<sup>IN</sup> remaining after 120 minutes is expressed as the standard deviation.

#### **Maximum extra-membrane hydrophilicity analysis**

The UniprotKB/SwissProt database was downloaded on 11/15/2016. Membrane proteins were identified as marked TRANSMEM in the FT line. Only proteins with three or more transmembrane helices were used in the analysis. All amino acids in the sequence not marked TRANSMEM were considered extra-membrane. To determine the hydrophilicity of each extra-membrane segment, the hydrophobicity of each amino acid in the segment was summed using the biological hydrophobicity scale.<sup>26</sup> The most hydrophilic (least hydrophobic) extra-membrane segment was then defined as the maximum extra-membrane hydrophilicity of the protein.

#### **Acknowledgements**

The authors would like to thank members of the lab for helpful comments on the manuscript. This work was supported by NIH R01GM063919 to JUB and an NIH Chemistry/Biology Interface Training Grant to N.B.W.

#### **References**

1. Anglin TC, Liu J, Conboy JC (2007) Facile lipid flip-flop in a phospholipid bilayer induced by gramicidin A measured by sum-frequency vibrational spectroscopy. *Biophys J* 92:L01–L03.
2. Popot J-L, Engelman DM (1990) Membrane protein folding and oligomerization: the two-stage model. *Biochemistry* 29:4031–4037.
3. von Heijne G (1986) The distribution of positively charged residues in bacterial inner membrane proteins correlates with the trans-membrane topology. *EMBO J* 5:3021.
4. Lu Y, Turnbull IR, Bragin A, Carveth K, Verkman AS, Skach WR (2000) Reorientation of aquaporin-1 topology during maturation in the endoplasmic reticulum. *Mol Biol Cell* 11:2973–2985.
5. Bogdanov M, Heacock PN, Dowhan W (2002) A polytopic membrane protein displays a reversible topology dependent on membrane lipid composition. *EMBO J* 21:2107–2116.
6. Vitrac H, Bogdanov M, Heacock P, Dowhan W (2011) Lipids and topological rules of membrane protein assembly: Balance between long and short range lipid-protein interactions. *J Biol Chem* 286:15182–15194.
7. Vitrac H, Bogdanov M, Dowhan W (2013) In vitro reconstitution of lipid-dependent dual topology and postassembly topological switching of a membrane protein. *Proc Natl Acad Sci USA* 110:9338–9343.
8. Vitrac H, MacLean DM, Jayaraman V, Bogdanov M, Dowhan W (2015) Dynamic membrane protein topological switching upon changes in phospholipid environment. *Proc Natl Acad Sci USA* 112:13874–13879.
9. Serdiuk T, Sugihara J, Mari SA, Kaback HR, Müller DJ (2015) Observing a lipid-dependent alteration in single lactose permeases. *Structure* 23:754–761.

10. Woodall NB, Yin Y, Bowie JU (2015) Dual-topology insertion of a dual-topology membrane protein. *Nat Commun* 6:8099.
11. Chen Y-J, Pornillos O, Lieu S, Ma C, Chen AP, Chang G (2007) X-ray structure of EmrE supports dual topology model. *Proc Natl Acad Sci USA* 104:18999–19004.
12. Morrison EA, DeKoster GT, Dutta S, Vafabakhsh R, Clarkson MW, Bahl A, Kern D, Ha T, Henzler-Wildman KA. (2011) Antiparallel EmrE exports drugs by exchanging between asymmetric structures. *Nature* 481:45–50.
13. Soskine M, Steiner-Mordoch S, Schuldiner S (2002) Crosslinking of membrane-embedded cysteines reveals contact points in the EmrE oligomer. *Proc Natl Acad Sci USA* 99:12043–12048.
14. Soskine M, Mark S, Tayer N, Mizrahi R, Schuldiner S (2006) On parallel and antiparallel topology of a homodimeric multidrug transporter. *J Biol Chem* 281:36205–36212.
15. Schuldiner S (2007) When biochemistry meets structural biology: the cautionary tale of EmrE. *Trends Biochem Sci* 32:252–258.
16. Schuldiner S (2009) EmrE, a model for studying evolution and mechanism of ion-coupled transporters. *Biochim Biophys Acta* 1794:748–762.
17. Nasie I, Steiner-Mordoch S, Gold A, Schuldiner S (2010) Topologically random insertion of EmrE supports a pathway for evolution of inverted repeats in ion-coupled transporters. *J Biol Chem* 285:15234–15244.
18. Lloris-Garcera P, Bianchi F, Slusky JSG, Seppala S, Daley DO, von Heijne G (2012) Antiparallel dimers of the small multidrug resistance protein EmrE are more stable than parallel dimers. *J Biol Chem* 287:26052–26059.
19. Lloris-Garcera P, Slusky JSG, Seppälä S, Prieß M, Schäfer LV, von Heijne G (2013) In vivo Trp scanning of the small multidrug resistance protein EmrE confirms 3D structure models. *J Mol Biol* 425:4642–4651.
20. Rapp M, Seppala S, Granseth E, von Heijne G (2007) Emulating membrane protein evolution by rational design. *Science* 315:1282–1284.
21. Seppala S, Slusky JS, Lloris-Garcera P, Rapp M, von Heijne G (2010) Control of membrane protein topology by a single C-terminal residue. *Science* 328:1698–1700.
22. Zhu Q, Casey JR (2007) Topology of transmembrane proteins by scanning cysteine accessibility mutagenesis methodology. *Methods* 41:439–450.
23. Muth TR, Schuldiner S (2000) A membrane-embedded glutamate is required for ligand binding to the multidrug transporter EmrE. *EMBO J* 19:234–240.
24. Herman C, Prakash S, Lu CZ, Matouschek A, Gross CA (2003) Lack of a robust unfoldase activity confers a unique level of substrate specificity to the universal AAA protease FtsH. *Mol Cell* 11:659–669.
25. Van Lehn RC, Zhang B, Miller IIITF (2015) Regulation of multispinning membrane protein topology via post-translational annealing. *eLife* 4:e08697.
26. Hessa T, Kim H, Bihlmaier K, Lundin C, Boekel J, Andersson H, *et al.* (2005) Recognition of transmembrane helices by the endoplasmic reticulum translocon. *Nature* 433:377–381.
27. Rapp M, Granseth E, Seppälä S, Von Heijne G (2006) Identification and evolution of dual-topology membrane proteins. *Nat Struct Mol Biol* 13:112–116.
28. Dutzler R, Campbell EB, Cadene M, Chait BT, MacKinnon R (2002) X-ray structure of a Cl<sup>-</sup> channel at 3.0 Å reveals the molecular basis of anion selectivity. *Nature* 415:287–294.
29. Kapust RB, Waugh DS (2000) Controlled intracellular processing of fusion proteins by TEV protease. *Protein Expr Purif* 19:312–318.
30. Ogura T, Inoue K, Tatsuta T, Suzaki T, Karata K, Young K, Su LH, Fierke CA, Jackman JE, Raetz CR, Coleman J, Tomoyasu T, Matsuzawa H. (1999) Balanced biosynthesis of major membrane components through regulated degradation of the committed enzyme of lipid A biosynthesis by the AAA protease FtsH (HflB) in *Escherichia coli*. *Mol Microbiol* 31:833–844.